PHYSICAL REVIEW B VOLUME 27, NUMBER 6 15 MARCH 1983

X-ray absorption spectroscopy of layer transition-metal disulfides

Y. Ohno, K. Hirama, S. Nakai, and C. Sugiura
Department of Applied Physics, Faculty of Engineering, Utsunomiya University, Ishii-machi 2753, Utsunomiya, Japan

S. Okada
Department of Physics, Faculty of General Education, Utsunomiya University, Mine-machi 350, Utsunomiya, Japan
(Received 1 June 1982)

We have measured the x-ray K absorption spectra of S and the L_{III} absorption spectra of Nb and Mo in layer transition-metal disulfides (TiS_2, VS_2, ZrS_2, NbS_2, MoS_2, and HfS_2), using a Yohan-type curved-crystal spectrometer. These spectra reflect the electronic band structures of these materials very well and exhibit the large peak originating in the empty "d" bands and the broad peak originating in the "metal sp" bands. In combination with the photoemission spectra and the band calculations, we obtain information on detailed band structures of both occupied and empty states, which were not inconsistent with the other experimental results, such as the reflectivity and the energy-loss spectra. We could also obtain information on band character, owing to the selection rules and the localization property of an x-ray spectrum. The results obtained suggest the strong covalency of these materials.

I. INTRODUCTION

The group-IV, -V, and -VI transition metals (T) yield many layer compounds (TS_2) in combination with sulfur (S). There are two different types of coordination of a metal atom in these compounds: One is octahedral coordination and the other is trigonal prismatic coordination. A sixfold S-T-S sandwich layer is constructed of a two-dimensional arrangement of T and S atoms and a three-dimensional crystal is composed of the regular stacking of S-T-S sandwich layers. The different stacking sequence of the same or different type of layers yields various polymorph and polytypes for these compounds. The bonding between the layers is believed to be due to the van der Waals force, so that the interlayer interaction does not so heavily affect the electronic band structure. As a result, the electric, magnetic, and optical properties of these materials exhibit a two dimensionality or a three dimensionality having a strong anisotropy.

Several energy-band models[1-4] have been proposed for these compounds, most of which are, however, modifications of Wilson and Yoffe's model.[5] In their model the d bands split by ligand field exist in the energy gap between the bonding σ band derived primarily from S p orbitals and the antibonding σ^* band derived from transition-metal s and p orbitals. Wilson and Yoffe also suggested the application of a rigid-band model to the electronic band structures of a series of layer transition-metal dichalcogenides. Thereafter, many band calculations[6] have been performed and all of them roughly support Wilson and Yoffe's model in spite of different methods of calculation and different materials. However, there have also occurred some modifications in detail. For example, the lower d band overlaps the bonding σ band in compounds such as MoS_2 and $NbSe_2$,[7] and the large d-band separation of the materials with a trigonal prismatic structure is caused by the hybridization of d orbitals rather than by the ligand-field splitting.[8] The experimental information on the filled states of these compounds has been obtained from photoemission spectra,[9-12] while information on the joint density of states between the valence and conduction bands has been obtained from reflectivity,[13,14] transmission,[15] and the energy-loss spectra.[16] Knowledge of the empty states is, however, relatively scarce to date.

Although an x-ray spectrum is inferior to other optical spectra in resolving power, it gives information on both filled (emission) and empty (absorption) states separately over a wide energy range.

One also obtains information on the band character and the kind of orbitals constituting a band, owing to the selection rules. As core levels participate in electronic transition processes of x-ray emission or absorption, if charge transfer occurs in forming a compound, the absorption edge is shifted to lower or higher energies. Hence, we can also obtain information on bonding states involving charge transfer by analyzing the shift of the absorption edge or the peak positions. The following x-ray spectroscopies have been performed for layer TS_2 compounds: (a) the emission and absorption spectra of TiS_2,[17] (b) the MoL_{III} absorption spectrum[18] and a series of emission spectra[19,20] of MoS_2, (c) the S$L_{II,III}$ absorption spectra of TiS_2, MoS_2, and TaS_2,[21] (d) the VK absorption spectrum of VS_2,[22] and (e) the TaL_{III} absorption spectrum of TaS_2.[23,24] Almost all absorption spectra obtained by Fischer[17] were self-absorption replicas, while the spectra obtained by Sonntag *et al.*[21] exhibited the overlap of two absorptions originating in a spin-orbit splitting pair of core levels.

In the present paper, we discuss the SK absorption spectra of a series of layer TS_2 compounds, comparing with the VK, NbL_{III}, and MoL_{III} absorption spectra and the other experimental results such as photoemission, reflectivity, and energy-loss spectra. We compare experimental results with the theoretical band calculations. Finally, we describe the band structure of these compounds together with the contribution of atomic orbitals to each band.

II. EXPERIMENT

All the samples except for the natural molybdenite were prepared by high-temperature reaction from elements in stoichiometric amounts in evacuated silica ampoules with inner diameter 1.5 cm and length 30 cm. The samples were investigated by x-ray powder patterns. The determination of the lattice parameters and the Miller indices was performed with the use of a computer. It was possible to assign Miller indices to almost all difffraction peaks.

The measurements of x-ray absorption spectra except for VK were done with the use of a Yohan type of vacuum soft x-ray spectrometer having a Rowland circle with radius 30 cm. The samples to be investigated were prepared in the form of a thin film by rubbing fine powder onto a sheet of thin paper. The dispersing crystal was quartz with a $(10\bar{1}1)$ plane for SK and MoL_{III} spectra and with a $(10\bar{1}0)$ plane for NbL_{III} spectra, respectively. The operating conditions of the x-ray tube were 4.3 kV and 30 mA with a tungsten anode. The x rays penetrating a sample were dipersed by the quartz crystal and detected by a gas-flow proportional counter using a 90 vol % argon—10 vol % methane mixture as flow gas. The detected photon signals passing through a preamplifier and a pulse height analyzer were integrated by a scaler during a preset time and then were printed out automatically on both a printer and a recorder. The total spectrum was obtained by step scanning. The one-step energies of SK, MoL_{III}, and NbL_{III} spectra were 0.290, 0.300, and 0.323 eV, respectively. The final spectrum was drawn on an X-Y plotter in the form of a normalized optical density as a function of energy by accumulating three to six data sets for each material and processing them with a computer. In obtaining the absolute photon energies, we used the energy values of Mo$L\alpha_1$, $L\beta_1$, $L\beta_3$, and $L\beta_{4,6}$ lines given in Bearden's x-ray wavelength table[25] and the SK absorption peak energy of $CaSO_4 \cdot 2H_2O$ given by Sugiura *et al.*[26]

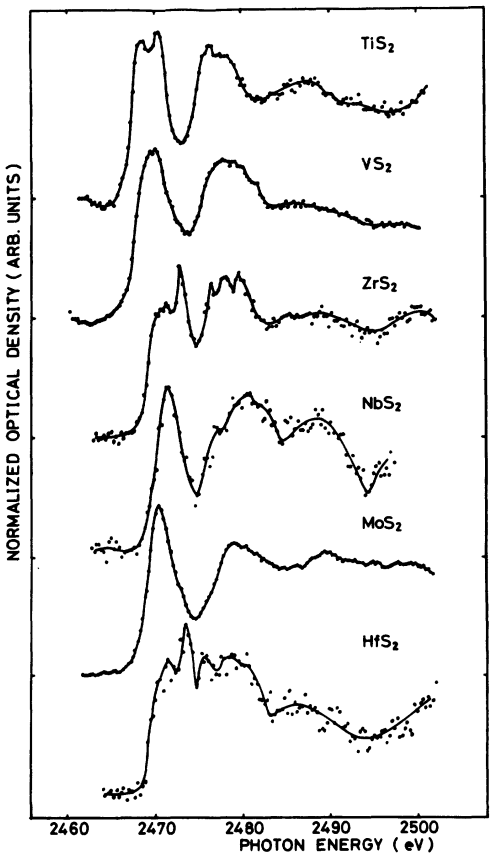

FIG. 1. SK absorption spectra of a series of layer transition-metal disulfides.

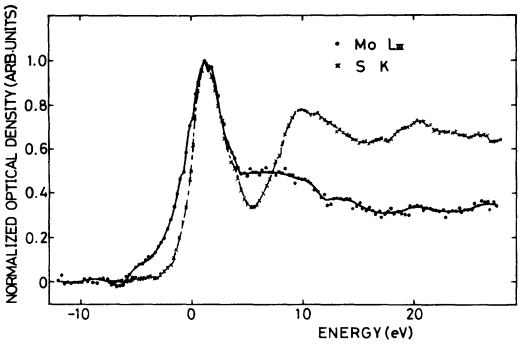

FIG. 2. Mo L_{III} and S K absorption spectra of MoS_2.

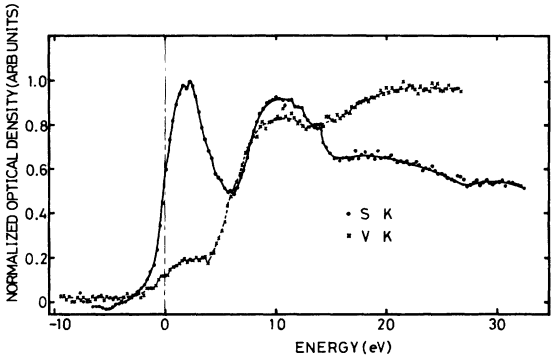

FIG. 3. V K and S K absorption spectra of VS_2.

III. RESULTS AND DISCUSSIONS

Figure 1 shows the S K absorption spectra of a series of layer TS_2 compounds. These spectra are similar to each other in shape, especially, for the materials with the same crystal structure. TiS_2, ZrS_2, HfS_2, and VS_2 crystallize in an octahedral structure, while NbS_2 and MoS_2 in a trigonal prismatic structure. As an x-ray absorption spectrum reflects the empty states, Fig. 1 suggests the similarity of the empty-band structure of these materials. Before discussing the absorption spectrum and the electronic band structure of each material, we will compare the different spectra of the same material.

Figure 2 shows a comparison between the Mo L_{III} and S K absorption spectra of MoS_2. As an L_{III} absorption spectrum, in general, reflects the empty states with s and d character (s and d symmetry), while a K absorption spectrum reflects the empty states with p character, so it is found that the structures from the absorption edge (the middle point of the initial rise) to about 5 eV are primarily due to the bands of admixed p and d orbitals, while the structures from 6 to 14 eV are primarily due to the admixed s and p orbitals. Figure 3 shows a comparison between the V K and S K absorption spectra of VS_2. It is found from these spectra that the former p character is derived predominantly from S p orbitals, while the latter p character is derived from both metal and S p orbitals. This inference assumes the localized property of an x-ray excitation. Finally, these bands are found to correspond to the d and metal sp bands generally called for in the band structure of these materials.

A. The group-IV TS_2 compounds (TiS_2, ZrS_2, and HfS_2)

The energies of the absorption edge of TiS_2, ZrS_2, and HfS_2 are 2467.4, 2469.1, and 2469.2 eV, respectively, and shift to higher energies while going from TiS_2 to ZrS_2 and then HfS_2. This shift cannot be explained by the chemical shift. Since the S atom behaves as an anion in these compounds and their ionicity increases with the atomic number of a transition metal, the charge density around a S ion increases in the sequence. As a result, the shielding of core electrons against a nucleus increases while going from TiS_2 to HfS_2, and the binding energies of core levels and the absorption edge are shifted to lower energies in the sequence contrary to our experimental results. It is well known that ZrS_2 and

TABLE I. Energies from the absorption edge to the main structures of S K spectra of layer transition-metal disulfides. Notations are given in Figs. 4–7, 9, and 10. ΔE_0 is the energy shift of the absorption edge and the results are given in eV.

Materials	O	A'	A	B	C'	C	C''	D	E	F	ΔE_0
TiS_2	0	1.3	3.3	5.8	9.2	10.5		14.9	20.1	20.2	0
ZrS_2	0	1.9	3.4	5.4	6.9	8.6	10.2	14.0	19.4	25.1	+1.9
HfS_2	0	1.6	3.6	4.7	5.4	8.6		13.4		24.3	+2.4
VS_2	0	1.8	2.6	6.1		10.2	11.6	16.0			+0.4
NbS_2	0		1.4	4.7	7.4	10.5		14.4	18.4	24.0	+2.6
MoS_2	0		1.4	5.6		10.0	11.4	15.4	20.4		+2.0

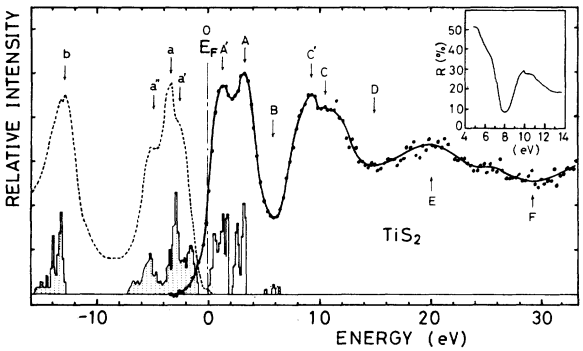

FIG. 4. SK absorption spectrum of TiS_2, together with the photoemission spectrum measured by Wertheim *et al.* (Ref. 9) and the density of states calculated by Bullett (Ref. 32). Inset is the reflectivity measured by Hughes and Liang (Ref. 14).

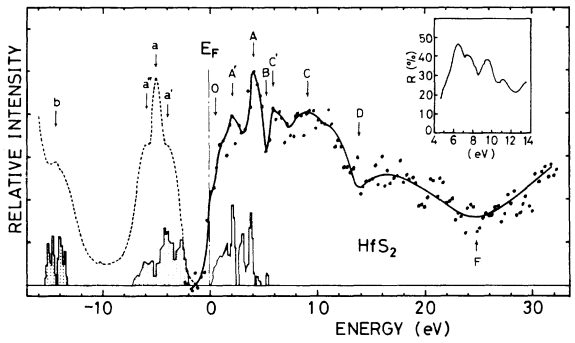

FIG. 5. SK absorption spectrum of ZrS_2, together with the photoemission spectrum measured by Wertheim *et al.* (Ref. 9) and the density of states calculated by Bullett (Ref. 32). Inset is the reflectivity measured by Hughes and Liang (Ref. 14).

HfS_2 are n-type semiconductors with a band gap of 1.7 and 2.0 eV, respectively.[13] It is uncertain whether TiS_2 is a narrow-gap semiconductor or a semimetal. However, all band-structure calculations[27–30] to date suggest that it is a semiconductor. In addition, the angle-resolved photoemission data obtained by Chen *et al.*[31] also showed that TiS_2 is a narrow-gap semiconductor with a band gap of 0.3 ± 0.2 eV. According to the band-structure calculation by Bullett,[32] on the other hand, the energies of the lowest empty state of TiS_2, ZrS_2, and HfS_2 are -8.0, -7.3, and -7.0 eV, respectively, increasing while going from TiS_2 to HfS_2. In the light of these facts, it is concluded that the shift of the absorption edge of these spectra may result from the final states or the empty states. The energies of the main structures of these spectra are summarized in Table I. These energies are measured from the absorption edge. The relative intensity of the first peak in the SK absorption spectrum of TiS_2 is large, compared with that obtained by Fischer.[17]

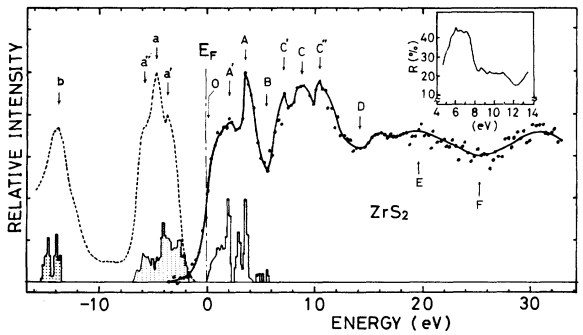

FIG. 6. SK absorption spectrum of HfS_2, together with the photoemission spectrum measured by Wertheim *et al.* (Ref. 9) and the density of states calculated by Bullett (Ref. 32). Inset is the reflectivity measured by Hughes and Liang (Ref. 14).

Figures 4, 5, and 6 show the SK absorption spectra of TiS_2, ZrS_2, and HfS_2, respectively, together with the x-ray photoemission spectrum measured by Wertheim *et al.*[9] and the density of states calculated by Bullett.[32] The insets in Figs. 4–6 show the reflectivity spectra obtained by Hughes and Liang.[14] The origin of the horizontal axis is the Fermi energy estimated from the photoemission study. The density of states diagram has been plotted on the figures by fitting its peak position to that of the photoemission spectrum as well as possible and then the SK absorption has been plotted on the figures by fitting its peak position to that of the density of states. The reason why we used the x-ray photoemission spectra measured by Wertheim *et al.* is that the width of the valence band can be estimated more accurately, compared with the ultraviolet photoemission spectra, because the influences of the multielectron processes such as plasmons and the other electronic excitations and of the final-state modulation are smaller. The reasons why we particularly used Bullett's results among many band-structure calculations of these materials are as follows: (i) His results for TiS_2 agree well with those of Zunger and Freeman,[30] who have calculated self-consistently, and further with the photoemission spectrum measured by Wertheim *et al.*[9] (ii) It is possible to discuss our experimental results systematically, comparing with his results, because he has calculated the band structures and the density of states of a series of layer transition-metal dichalcogenides. As a result, there is good agreement between theory and experiment. The Fermi level, in all cases, exists in the energy gap near the bottom of

the conduction band. This result coincides with the fact that ZrS_2 and HfS_2 are n-type semiconductors and TiS_2 is also expected to be a degenerate n-type semiconductor. The absorption edge is found to be situated at the bottom of the conduction band as predicted. In addition, we can also obtain the following information from Figs. 4—6:

(a) The peaks A' and A of the S K absorption spectra correspond to two peaks of the density of states which are well known as t_{2g} and e_g bands. We can estimate from the peak distance that the t_{2g}-e_g band splitting of TiS_2, ZrS_2, and HfS_2 is 2.0, 1.5, and 2.0 eV, respectively. The value for TiS_2 is approximately equal to that obtained by Fischer[17] (2.1 eV), Webb *et al.*[33] (2.2 eV), and Sonntag *et al.*[21] (2.3 eV).

(b) There is considerable p character even in the t_{2g} and e_g bands. This p character is derived primarily from S p orbitals. This result suggests the presence of the strong admixture of transition-metal d and S p orbitals, in other words, the strong covalent bonding between metal and S atoms.

(c) We could not accurately estimate the d-band width because of the comparatively low resolution of the x-ray spectra due to the broadening of a core level and because of the overlap with metal sp bands situated at the higher-energy side. Assuming the energy distance between the absorption edge and the middle point between A and B to be the d-band width, however, it is 4.1, 4.6, and 5.0 eV for TiS_2, ZrS_2, and HfS_2, respectively, which are larger than the theoretical values obtained by Bullett[32] by about 0.8 eV.

(d) The extent of the overlap between the d and metal sp bands increases with the atomic number of a transition metal. According to Bullett,[32] the d level at d^2 configuration increases, compared with the other levels, while going from Ti to Hf, and the d bands separate from the metal sp bands by a gap for TiS_2, but they are degenerate for ZrS_2 and HfS_2. Therefore, it may be expected that the energy position of d levels plays an important role for the overlap between the d and metal sp bands and for the semiconductor gap.

(e) The width of the metal sp bands is estimated to be about 8 eV.

(f) The valence band consists of the lower bands (chalcogen s bands) situated at 13—15 eV below the Fermi level and of the upper bands (chalcogen p bands) having a main peak at a center and shoulder or small peak structures on both sides.

The reflectivities and the joint densities of states derived from the energy-loss spectra of ZrS_2 and HfS_2 exhibit large peaks around 3 and 7 eV together with a large dip around 4 eV. From Figs. 5 and 6, interband transitions of these materials are expected to arise at about 2 eV. Considering the relatively wide upper valence band, about 5-eV wide, and the relatively small t_{2g}-e_g band splitting, however, it is impossible to predict a sharp peak around 3 eV and a large dip around 4 eV from the density of states. In relating with this point, Isomäki and Boehm[34] have indicated the importance of the matrix-element effect on ϵ_2, the imaginary part of the dielectric constant. The peak around 6 eV and the dip around 12 eV, on the other hand, can be sufficiently explained in terms of only the density of states. The former is caused by the chalcogen $p-d$

TABLE II. Relations between the main energy distances in Figs. 4—6 and the peak energies of the corresponding reflectivity given by Greenaway and Nitsche (Ref. 13) and Hughes and Liang (Ref. 14). The former data are in parentheses and the results are given in eV.

	Main energy distances			Reflectivity-peak energies		
Notations	TiS_2	ZrS_2	HfS_2	TiS_2	ZrS_2	HfS_2
				(1.95)	(2.75)	(2.9)
				(2.2)	(3.3)	(3.35)
a'-O	2.6	3.8	4.4			
a-O	3.4	4.9	5.4	(3.35)	4.97(4.7)	5.0(5.00)
a'-A'	4.0	5.7	6.0		5.7	
a''-O	4.9	5.9	6.4	(4.5)	6.07(6.1)	6.46(6.40)
a-A'	4.8	6.8	7.0	4.94(5.0)	6.6	
					7.1	
a'-A	5.8	7.3	8.0		7.36(7.3)	7.87(7.9)
a''-A'	6.3	7.8	8.0			
						8.67
						8.98
a-A	6.6	8.4	9.0	6.72(6.8)	8.57(8.7)	9.34(9.35)
a''-A	8.1	9.3	9.9		9.56	9.6

interband transitions and the latter is caused by both the reduced chalcogen $p-d$ interband transitions and the increase of the chalcogen $p-$metal sp interband transitions. The main energy distances in Figs. 4–6 are connected with the peak energies of the reflectivity of the corresponding material in Table II. There is a comparatively good agreement between them, but a perfect coincidence cannot be obtained. This may be, of course, due to the imperfect coincidence between the convolution of the density of states of the valence and conduction bands and the joint densities of states.

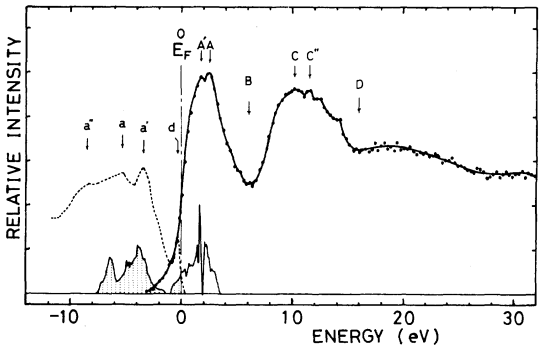

FIg. 7. S K absorption spectrum of VS_2, together with the photoemission spectrum of VSe_2 measured by Shepherd and Williams (Ref. 7) and the density of states calculated by Myron (Ref. 35).

B. The group-V TS_2 compounds

1. An octahedral coordination type (VS_2)

The V K absorption spectra of VS_2 and VSe_2 have been already reported in Ref. 22 by the present authors, in which their similarity has been emphasized. Figure 3 shows the V K and S K spectra, whose absorption edges are 5465.0 and 2467.8 eV, respectively, but the absolute energy values of the empty states cannot be obtained from only x-ray spectra. However, many structures are connected with each other by fitting the absorption edges. Figure 7 shows the S K absorption spectrum of VS_2, together with the photoemission spectrum of VSe_2 measured by Shepherd and Williams[11] and the density of states calculated by Myron,[35] with the use of the augmented-plane-wave (APW) method. It is found that the absorption edge coincides with the Fermi level present in the d band and the peaks A' and A of the S K absorption spectrum correspond to two peaks of the density of states as well as the group-IV TS_2 compounds. The structures to about 5 eV above the absorption edge reflect the d bands and the structures from 6 to 14 eV reflect the metal sp bands. We can obtain the following information from Figs. 3 and 7:

(a) The d bands are derived primarily from V d and S p orbitals.

(b) The metal sp bands are derived primarily from V and S s and p orbitals.

(c) The ligand-field splitting is observed, but is small, compared with those of the group-IV TS_2 compounds. The whole appearance of the S K spectrum comes to resemble those of MoS_2 and NbS_2 having a trigonal prismatic structure.

(d) From the photoemission spectrum of VSe_2, we may expect some overlap between the chalcogen p and d bands as well as $NbSe_2$ and MoS_2 described below.

As mentioned above, there are two different types of coordination in the crystal structure of layer TS_2 compounds: octahedral and trigonal prismatic coordination. Wilson and Yoffe[5] suggested that the type of coordination depends on the number of electrons that occupy the d bands. Trigonal prismatic coordination gives rise to a large d-band separation due to both the ligand field and the hybridization of d orbitals, and the lower d band allows occupation by two electrons. To date it is believed that the electronic occupation of this band is the driving force toward the trigonal prismatic structure. As a result, the group-V and -VI TS_2 compounds are stabilized for a trigonal prismatic structure because there are one or two electrons in the band, while the group-IV TS_2 compounds are stabilized for the more symmetric, electrostatically favored, octahedral structure because there are no electrons in the band. In practice, TiS_2, ZrS_2, and HfS_2 crystallize in the octahedral structure, while NbS_2 and MoS_2 crystallize in the trigonal prismatic structure. Vanadium dichalcogenides, which belong to the group-V transition-metal dichalcogenides, however, crystallize in the octahedral structure. This fact may imply the comparatively low-energy gain in the trigonal prismatic structure for these materials, which seems to be related to the above-mentioned results (c) and (d). Especially, it appears that the overlap between the chalcogen p and d bands play an important role for the stabilization of the octahedral structure of these materials. In relation to this problem, it is interesting to note that their lattice-parameter ratios (c/a) are in the neighborhood of those of MoS_2 and NbS_2 rather than those of the group-IV TS_2 compounds.[36]

2. *A trigonal prismatic coordination type (NbS_2)*

The S K absorption edge of NbS_2 is situated near the Nb L_{II} absorption edge, and these spectra overlap as shown in Fig. 8(a). According to Bearden's x-ray wavelength table,[23] the energies of S K and Nb L_{II} absorption edges are 2470.48 and 2464.1 eV, respectively. If the Nb L_{III} absorption spectrum ($2p_{3/2} \rightarrow$ empty s and d states) is the same shape as the L_{II} spectrum ($2p_{1/2} \rightarrow$ empty s and d states), we can pick up only the S K absorption spectrum by fitting the first peak of the Nb L_{III} spectrum shown in Fig. 8(b) to that of the raw spectrum shown in Fig. 8(a) and then subtracting the former from the latter. Figure 8(c) shows the normalized S K absorption spectrum of NbS_2 obtained in this way. This spectrum is found to be similar to the S K absorption spectrum of MoS_2 shown in Fig. 2. Although the first large peaks of Figs. 8(b) and 8(c) originate in the same bands, the width of the former peak is larger than that of the latter peak. The same phenomenon is observed in the corresponding absorption spectra of MoS_2 and is probably due to the difference in the broadening of core levels or due to the core-hole—metal-4d-electron interaction.

Figure 9 shows the S K absorption spectrum of NbS_2, together with the photoemission spectrum[9] of $NbSe_2$ and the density of states.[32] The Nb L_{III} absorption spectra of NbS_2 and $NbSe_2$ resemble each other and the electronic band structures of these compounds are quite similar to each other. The absorption edge of the S K spectrum coincides with the bottom of the conduction band situated at 1 eV above the Fermi level. In this case, the Fermi level exists in the d_{z^2} band, so that we may expect two absorption peaks originating in the empty d_{z^2} band and the rest d bands. However, we can observe only a large peak having a shoulder structure at the lower-energy side of the absorption edge because of the broadening of the S 1s level. It appears that the shoulder structure reflects the empty d_{z^2} band. We can obtain the following information from Figs. 8 and 9:

(a) The peak A reflects the bands of admixed Nb d and S p orbitals.

(b) The peaks C' and C reflect the bands of admixed Nb and S s and p orbitals. The former is more s-like and the latter is more p-like.

(c) The band structures of NbS_2 and $NbSe_2$ are similar to that of MoS_2 as expected from the rigid-band model. According to the band calculations,[8,32] there is a large gap between the d and metal sp bands. However, our experimental results suggest the overlap of these bands.

(d) The sharp peak, which is observed at 4.4 eV in the reflectivity[14] and the joint density of states from the energy-loss spectrum[16] of $NbSe_2$, corresponds to the chalcogen $p-d$ interband transitions between a' and A, while the dip around 8 eV may correspond to both the reduced chalcogen $p-d$ interband transitions and the increase of the chalcogen p—metal sp interband transitions because the energy distances between a'' and A and between d and C' are about 8 eV.

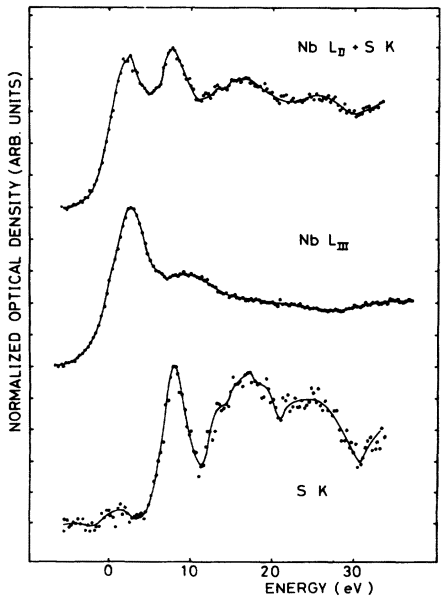

FIG. 8. X-ray absorption spectra of NbS_2; (a) Nb L_{II} and S K spectra, (b) Nb L_{III} spectrum, and (c) S K spectrum.

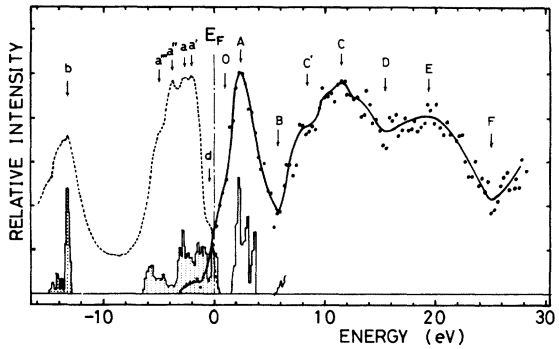

FIG. 9. S K absorption spectrum of NbS_2, together with the photoemission spectrum of $NbSe_2$ measured by Wertheim *et al.* (Ref. 9) and the density of states calculated by Bullett (Ref. 32).

C. The group-VI TS_2 compounds (MoS_2)

The Mo L_{III} and S K absorption spectra of MoS_2 are shown in Fig. 2. The Mo L_{III} spectrum is different from that of Barinski and Vainshtein[18] in shape. They have observed a large additional peak at the lower energy side of the absorption edge. However, the present Mo L_{III} absorption spectrum resembles the Nb L_{III} absorption spectra of NbS_2 and $NbSe_2$ and consists of only a large peak followed by a broad structure. These spectra have been already discussed in other sections of this paper and suggest the strong covalency of these materials. Haycock *et al.*[20] measured the Mo $L\beta_{2,15}$, Mo_{5p-3d}, S $K\beta_{1,3}$, and S $L_{1,\eta}$ emission spectra and indicated the strong covalent between Mo and S atoms, in agreement with our conclusions. Exciton peaks are observed in optical spectra of the group-VI transition-metal dichalcogenides[5] and are interpreted to be due to the *d-d* interband transitions in spite of the forbidden ones. However, if these bands are an admixture of metal *d* and chalcogen *p* orbitals, the exciton peaks would be caused by the allowed *p-d* or *d-p* transitions between the occupied and empty *d* bands.

Figure 10 shows the S K absorption spectrum of MoS_2, together with the photoemission spectrum measured by Wertheim *et al.*[9] and the density of states calculated by Bullett.[32] The absorption edge and the Fermi level, in this case, are situated within the band gap near the bottom of the empty *d* bands. This corresponds to the fact that MoS_2 is the *n*-type semiconductor with a gap of 1—2 eV. The reflectivity[14] and the joint density of states derived from the energy-loss spectrum[16] give rise to the prominent dip around 9 eV. This dip may be due to both the reduced chalcogen $p-d$ interband transitions

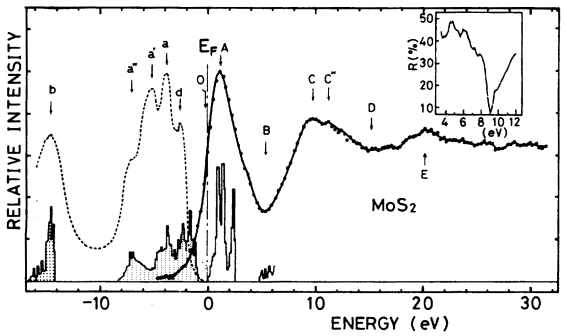

FIG. 10. S K absorption spectrum of MoS_2, together with the photoemission spectrum measured by Wertheim *et al.* (Ref. 9) and the density of states calculated by Bullett (Ref. 32). Inset is the reflectivity measured by Liang (Ref. 14).

TABLE III. Relations between the main energy distances in Fig. 10 and the peak energies of the reflectivity of MoS_2 given by Liang (Ref. 14). The results are given in eV.

Main energy distances		Reflectivity-peak energies
Notations	MoS_2	MoS_2
d''-O	2.4	
d-A	3.7	
		3.87
a-O	3.8	
		4.59
a'-O	4.9	
		4.86
a-A	5.0	
		5.46
		6.08
a'-A	6.4	6.25
a''-O	6.8	7.3
a''-A	8.2	7.9
d-B	7.9	
a-B	9.1	

and the increase of the occupied d—metal *sp* interband transitions because the energy distances between *a''* and *A* and between *d* and *B* are about 8 eV. However, the *s* part of the metal *sp* bands overlaps the unoccupied *d* bands, so that the chalcogen $p-s$ interband transitions occur even at this energy range. The fine structures around 4 eV may reflect the valence-band structure because the conduction band of this energy range consists of only a large peak. The energy relations are summarized in Table III.

IV. CONCLUSIONS

A. Energy-band structures

Although we have discussed the x-ray absorption spectra and the electronic band structures of layer TS_2 compounds, using the band names which are generally used for these materials, that is, chalcogen *p*, *d*, and metal *sp* bands, this is not strictly appropriate because large admixture occurs between metal and S *s*, *p*, and *d* orbitals. Therefore, we summarize the band structures of these materials by indexing each band (BD) by a simple number.

1. The group-IV TS_2 compounds (TiS_2, ZrS_2, and HfS_2)

These materials are semiconductors and the Fermi level is situated within the band gap near the

bottom of the BD3 band as shown in Fig. 11(a). The valence band consists of BD1 and BD2 bands. The former is situated at 13–15 eV below the Fermi level and has a bandwidth of 2–3 eV, while the latter has a bandwidth of 4–5 eV consists of a large peak at the center and the shoulder or small peak structures on both sides. The conduction band consists of BD3, BD4, and BD5 bands. The BD3 and BD4 bands are generally called the t_{2g} and e_g bands, whose splitting is due to ligand field and is 2.0, 1.5, and 2.0 eV for TiS_2, ZrS_2, and HfS_2, respectively. The BD5 band is about 8-eV wide and overlaps the BD4 band. Its extent increases with the atomic number of a transition metal.

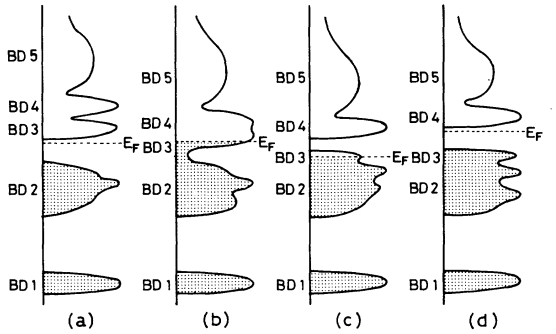

FIG. 11. Band-structure diagrams of layer transition-metal disulfides; (a) for the group-IV TS_2 compounds (b) for the group-V $1T$-TS_2 compounds, (c) for the group-V $2H(3R)$-TS_2 compounds, and (d) for the group-VI TS_2 compounds.

2. *The group-V 1T-TS_2 compound (VS_2)*

The valence band is quite similar to that of the group-IV TS_2 compounds, as shown in Fig. 11(b). As the group-V transition metal has an extra *d* electron, compared with the group-IV transition metal, the Fermi level exists in the BD3 band, which overlaps the BD2 band. It appears that this band overlap plays an important role for the stabilization of the octahedral structure of this group of materials, compensating the energy gain of trigonal prismatic coordination due to a large hybridization gap.

3. *The group-V 2H (3R)-TS_2 compounds (NbS_2)*

The Fermi level, in this case, exists in the BD3 band as well as the group-V $1T$-TS_2 compounds. The BD3 band overlaps the BD2 band, but separates from the BD4 band by the hybridization gap. It is believed that this hybridization gap is the driving force toward the trigonal prismatic structure of this group of materials as well as the group-VI transition-metal dichalcogenides. The widths of the BD2 and BD5 bands are comparable with those of the $1T$ compounds, but their shapes are slightly different. The BD4 band overlaps the *s* part of the BD5 band. The band structure of this group of materials is shown in Fig. 11(c).

4. *The group-VI TS_2 compounds (MoS_2)*

The electronic band structure of this group of materials is closely similar to that of group-V $2H$ $(3R)$-TS_2 compounds, excluding the position of the Fermi level, which exists in the band gap near the bottom of the BD4 band as shown in Fig. 11(d).

B. Band character

We can speculate on band character of these materials from a series of x-ray absorption spectra, adding a series of emisssion spectra obtained by Fischer[17] and Haycock *et al.*[20] The band names used to date are described in a parenthesis.

(a) BD1 band (chalcogen s band). This band is derived primarily from S *s* orbitals, but includes some *p* characteristics, also.

(b) BD2 band (chalcogen p or σ band). This band is derived from the admixture of S 3*p* and metal *s*, *p*, and *d* orbitals.

(c) BD3 band (d, t_{2g}, or d_{z^2} band). This band is derived from the strong admixture of metal *d* and S 3*p* orbitals.

(d) BD4 band (d or e_g band). This band is derived from the strong admixture of metal *d* and S 3*p* orbitals. However, some *s* character is also present.

(e) BD5 band (metal sp or σ^* band). This band is derived from the admixture of metal and S *s* and *p* orbitals.

[1]J. B. Goodenough, Mater. Res. Bull. 3, 409 (1968); Phys. Rev. 171, 466 (1968).
[2]R. Huisman, R. De Jonge, C. Haas, and F. Jellinek, J. Solid State Chem. 3, 56 (1971).
[3]M. G. Bell and W. Y. Liang, Adv. Phys. 25, 53 (1976).
[4]J. C. McMenamin and W. E. Spicer, Phys. Rev. B 16, 5474 (1977).
[5]J. A. Wilson and A. D. Yoffe, Adv. Phys. 18, 193 (1969).
[6]*Physics and Chemistry of Materials with Layered Struc-*

tures, edited by F. Levy (Reidel, Dordrecht, Holland, 1979), Vol. 3.
[7]F. R. Shepherd and P. M. Williams, J. Phys. C 7, 4427 (1974).
[8]L. F. Mattheiss, Phys. Rev. B 8, 3719 (1973).
[9]G. K. Wertheim, F. J. DiSalvo, and D. N. E. Buchanan, Solid State Commun. 13, 1225 (1973).
[10]J. C. McMenamin and W. E. Spicer, Phys. Rev. Lett. 29, 1501 (1972).
[11]F. R. Shepherd and P. M. Williams, J. Phys. C 6, L36 (1973); 7, 4416 (1974).
[12]N. V. Smith and M. M. Traum, Phys. Rev. B 11, 2087 (1975).
[12]D. L. Greenaway and Nitsche, J. Phys. Chem. Solids 26, 1445 (1965).
[14]H. P. Hughes and W. Y. Liang, J. Phys. C 10, 1079 (1977); W. Y. Liang, *ibid.* 4, L378 (1973).
[15]A. R. Beal, J. C. Knights, and W. Y. Liang, J. Phys. C 5, 3531 (1972).
[16]M. G. Bell and W. Y. Liang, Adv. Phys. 25, 53 (1976).
[17]D. W. Fischer, Phys. Rev. B 8, 3576 (1973).
[18]R. L. Barinski and E. E. Bainshtein, Izv. Akad. Nauk. SSSR Ser. Fiz. Mat. Nauk. 21, 1375 (1957).
[19]C. Sugiura, I. Suzuki, J. Kashiwakura, and Y. Gohshi, J. Phys. Soc. Jpn. 40, 1720 (1976).
[20]D. E. Haycock, D. S. Urch, and G. Wiech, J. Chem. Soc. Faraday Trans. 2, 75 (1979).
[21]B. Sonntag and F. C. Brown, Phys. Rev. B 10, 2300 (1974).
[22]Y. Ohno, H. Watanabe, A. Kawata, S. Nakai, and C. Sugiura, Phys. Rev. B 25, 815 (1982).
[23]S. V. Heald and E. A. Stern, Phys. Rev. B 16, 5549 (1977).
[24]J. Acrivos, S. S. P. Parkin, J. Code, J. Reynolds, K. Hathaway, H. Kurasaki, and E. A. Marseglia, J. Phys. C 14, L349 (1981).
[25]J. A. Bearden, Rev. Mod. Phys. 39, 78 (1967).
[26]C. Sugiura, Y. Fujino, and S. Kiyono, Tech. Rep. Tohoku Imp. Univ. 34, 125 (1969).
[27]R. B. Murray and A. D. Yoffe, J. Phys. C 5, 3038 (1972).
[28]H. W. Myron and A. J. Freeman, Phys. Lett. 44A, 167 (1973); Phys. Rev. B 9, 481 (1974).
[29]P. Krusius, J. von Boehm, and H. Isomäki, J. Phys. C 8, 3788 (1975).
[30]A. Zunger and A. J. Freeman, Phys. Rev. B 16, 906 (1977).
[31]C. H. Chen, W. Fabian, F. C. Brown, K. C. Woo, B. Davis, B. DeLong, and A. H. Thompson, Phys. Rev. B 21, 615 (1980).
[32]D. W. Bullett, J. Phys. C 11, 4501 (1978).
[33]C. Webb and P. M. Williams, Phys. Rev. B 11, 2082 (1975).
[34]H. M. Isomäki and J. von Boehm, J. Phys. C 14, L1043 (1981).
[35]H. W. Myron, Physica 99B, 243 (1980).
[36]F. G. Gamble, J. Solid State Chem. 9, 358 (1974).